A THz-TDS based metamaterial sensor for the sensitive distinguishment of food additives

MA Jia-Lu， TANG Jing-Chao， WANG Kai-Cheng， GUO Liang-Hao， WANG Shao-Meng， GONG Yu-Bin*

（School of Electronic Science and Engineering，University of Electronic Science and Technology of China，Chengdu 610054，China）

Abstract：A sensitive terahertz (THz) metamaterial sensor for the distinguishment of common additives in the food industry is proposed. The metamaterial sensor consists of an array of split ring resonator (SRR) with double tip ends. By checking resonate frequency shift of the sensor, the concentration and the type of the solution sample can be distinguished. The metamaterial sensor is fabricated on a quartz substrate, which is transparent for THz wave. The solutions with the concentration of 0. 2, 0. 4, 1. 5, 2, 3 and 4 mg/ml have been measured by using a terahertz time domain spectroscopy (THz-TDS). The results illustrate that the proposed metamaterial sensor can detect the concentration of the solution sample, as low as 0. 2 mg/ml. Meanwhile, different solutions with same concentration can also be clearly distinguished. Our study provides new insights for the application of terahertz metamaterial sensor based on SRR structure in the field of food safety.

Key words：terahertz sensor，metamaterial，TDS technology，highly sensitive，food safety

一种基于 THz−TDS 技术用于食品添加剂高灵敏度区分的超材料传感器

马佳路， 唐靖超， 王凯程， 郭良浩， 王少萌， 宫玉彬*

（电子科技大学 电子科学与工程学院，四川 成都 610054）

摘要：论文提出了一种用于食品工业中常用添加剂(肌醇、亮氨酸、牛磺酸)高灵敏度区分的太赫兹超材料传感器。该传感器由带有双尖端的开口谐振环(Split Ring Resonator, SRR)阵列组成。液体样品的不同浓度和种类对应于传感器不同的频率偏移，可以被用于液体样品浓度和种类的区分和辨别。该超材料传感器使用微纳工艺制作在对太赫兹波透明的石英基板上。利用太赫兹时域光谱仪(THz-TDS)系统分别测量了浓度为 0.2、0.4、1.5、2、3 和 4 mg/ml 的液体样品。结果表明，所提出的超材料传感器能检测的最低样品浓度为 0.2 mg/ml。同时，该传感器也可以实现相同浓度，不同种类液体样品的辨别。该研究为基于开口谐振环结构的太赫兹超材料传感器在食品安全领域的应用提供了新的参考。

关 键 词：太赫兹传感器；超材料；时域光谱技术；高灵敏度；食品安全

中图分类号：TN16　　　　　　　　　　　　　　　　**文献标识码**：A

Introduction

In the past decades，THz-TDS has been widely used in the biological，chemical and food safety fields[1-4]. Meanwhile，metamaterial，an artificial electromagnetic material with special electromagnetic characteristics，has been typically used for enhancing THz-material interactions to achieve high sensitivities. Generally，a metamaterial consists of periodic resonance elements providing enhancements on the electric field of specified frequency at certain locations of the sensor[5-9]. Terahertz sensors based on metamaterial have achieved more and more researchers' interest because of the full interactions between target samples and the enhanced electromagnetic waves. Any modification in the permittivity of the sample will lead to a clear signature in the electromagnetic response which could be recorded by using the THz-TDS. Thus，the THz sensor based on metamaterial can be utilized for the sensitive detection and distinction of biologi-

cal or chemical materials which have strong THz responses. Furthermore, the inter-molecular signatures in vast biological and chemical molecules are within the broad THz spectral bands[10-12].

With the rapid development of the food industry and the progress of chemical synthesis technology, food additives are widely used in the worldwide[13-15]. Inositol (IS) plays a specific role as the signaling molecule involves the regulation of vesicular trafficking as well as several other nuclear events[16-17]. Leucine (LC) and Taurine (TR) are also important amino acids that play important roles in human life activities[18-19]. IS, LC and TR have been widely added as food additive in the infant formula, health food and drink beverage because of the essential supplements for the human body[20-21]. The traditional detection methods for these food activities mainly include chemical methods, microbiological methods, spectroscopy methods, chromatography methods including gas chromatography, gas chromatography mass spectrometry, ion chromatography and liquid chromatography [22-26]. Terahertz detection technology provides the possibility to achieve high sensitivity, low cost and simple operation in the field of food activities. Especially, terahertz waves show great potential in bio-sensing applications because of the absorption of terahertz waves in these bio-molecular systems are pretty impressive.

In this paper, a terahertz sensor based on metamaterial which is composed of an array of double-gap SRR structure with tip ends has been proposed. The properties of the sensor are studied both numerically and experimentally. Meanwhile, the electric field distribution of the sensor with tip end has been studied. The sensing capability of the metamaterial sensor for the distinguishment of IS, LC and TR has been investigated by using the THz-TDS technology. The rapid and real-time monitoring of IS, LC and TR have been demonstrated based on the proposed metamaterial sensor. This method has the advantage of simple operation and low cost, which provide an effective reference for realizing the application of metamaterial in the field of food safety.

1 Materials and methods

1.1 Design and fabrication of the terahertz metamaterial sensor

The split ring resonator (SRR) with tip ends is selected as the metamaterial resonator element. Simulations were carried out by using Computer Software Technology (CST) Microwave Studio to study the high frequency properties of the metamaterial sensor. The schematic of the proposed metamaterial sensor is shown in Fig. 1, in which a 400 μm thick quartz wafer with the dielectric constant of 3.75 and loss tangent of 0.000 1 is used as the substrate. On the upper surface of the quartz substrate, a 200 nm thick gold with an electrical conductivity of 4.56 x 10^7 S/m is deposited to construct the resonators. The tip ends are created by cutting an ellipse off a circle that has the same center and cutting a rectangle with a long side of 140 μm parallel to the x direction. The radius of the circle is 70 μm, the major axis of the

ellipse is 136 μm, while the minor axis is 124 μm, the edge of the rectangle going across the center of the circle has a height of 12 μm. The incident THz wave was projected vertically onto the structure, with the E-field polarization perpendicular to the major axis of the proposed metamaterial structure. The inset of Fig. 1 shows the details of a single unit of the metamaterial sensor. The other optimized dimensional parameters of the single unit of the sensor are listed in Table 1.
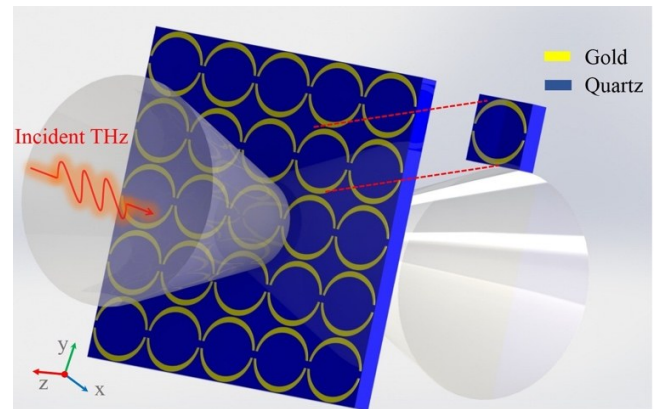

Fig. 1 The geometric diagram of the proposed metamaterial sensor based on SRR structure
图1 提出的基于开口谐振环结构的超材料传感器结构示意图

Table 1 Parameter values of the proposed metamaterial sensor
表1 超材料传感器结构参数

Parameters	Description	Values(μm)
a	The length of single unit	72
r	The radius of outer circle	70
l	The half of major axis	68
m	The half of minor axis	60
w	The height of rectangle	12

The simulation results of surface current and E-field distribution have been studied and shown in Fig. 2. The E-field polarization direction is parallel to the y-axis, as indicated by the red arrow in the figure. It can be observed that the electric field of SRR structure with tip ends becomes much stronger compared with ones without tip ends. Stronger E-field will lead more intense surface current accumulate at the tip ends, which means a higher sensitivity of the metamaterial sensor.

Then, the proposed metamaterial sensor based on SRR structure was fabricated by using semiconductor processing technology. Fig. 3 presents a typical optical microscopy image of the fabricated structure and the enlarged demonstration of unit cell.

1.2 Samples preparation and experiment setup

IS, LC and TR powder with a purity of 99.6% was purchased from Shanghai Macklin Biochemical Co., Ltd. The Deionized water was purchased form Chengdu Kelong Chemical Co., Ltd. Then, solutions to concentrations of 0.2 mg/ml, 0.4 mg/ml, 1.5 mg/ml, 2 mg/ml,
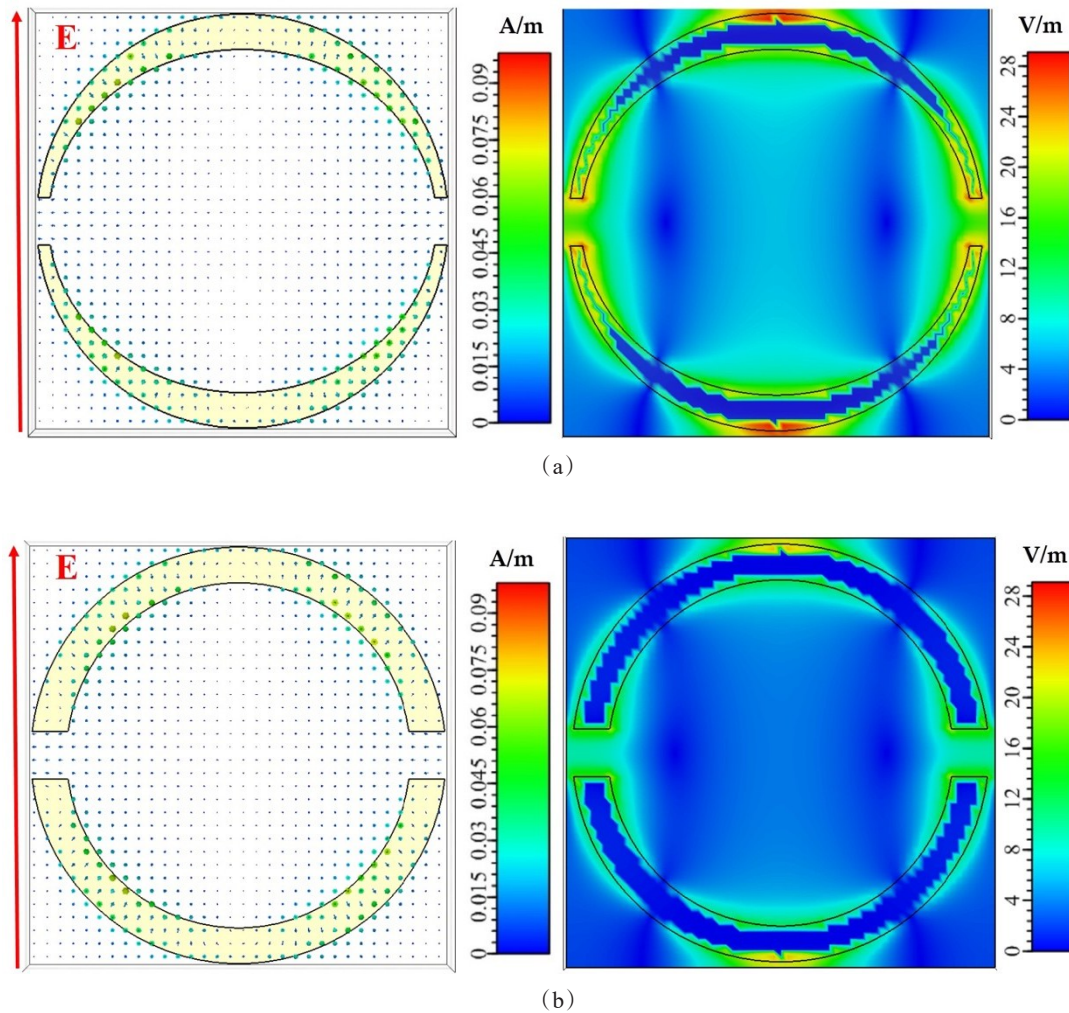
Fig. 2　The surface current and electric field profiles of SRR structure (a) with and (b) without tip ends, the red colored y-axis signifies the polarization direction of the incident electric field
图2　（a)有尖端和(b)没有尖端的开口谐振环结构表面电流和电场分布，红色y轴表示入射电场的极化方向

3 mg/ml and 4 mg/ml were obtained by mixing the IS，LC and TR powder and deionized water，respectively. We focused on these six solutions to concentrations ranging from 0. 2 to 4 mg/ml because it was found that the solution was beginning to crystallize when the concentration is greater than 4 mg/ml，leading to an uneven sample film when the water is evaporated. When the concentration of solution was lower than 0. 2 mg/ml，the sample thin film could not be detected due to the limited sensitivity of the proposed sensor and the limited frequency resolution of the TH-TDS.

The transmission spectra from 0. 01~6 THz were obtained by using the TH-TDS provided by Neaspace Company，which supplies 0. 01 THz resolution and 80dB dynamic range. The Ti：sapphire femtosecond laser was used to drive the THz-TDS system. The femtosecond laser beam was dived into pump and probe beam. The pump beam was incident on the photoconductive antenna to generate THz pulse. The generated THz pulse was collimated by parabolic mirrors and focused onto the mea-

surement area by using the 4-methyl-1-pentene（TPX） lens. The proposed metamaterial sensor was placed in the measurement area. Then，the transmitted THz signal through the sensor was measured by electro-optic sampling technique based on ZnTe crystal using time delay between the probe beam and the generated THz pulse. The measurement system is shown in Fig. 4（a-b），sensor assembled with fixture was placed into the holder to ensure the consistency of sensing position. During the experiment，THz time-domain spectra of samples were collected in transmission mode. All collections were carried out at room temperature and humidity less than 2%. The specific measurement process was as follows：firstly，the fabricated metamaterial sensor was cleaned with deionized water and dried with drying oven；then，the sensor was putted into a sample cell，and 10 μl sample solutions were dropped on the surface of the sensor by using Sartorius Mechanical Pipette；after that，the metamaterial sensor was placed into the drying oven for 20 minutes with the temperature at 60 °C to avoid any additional ab-
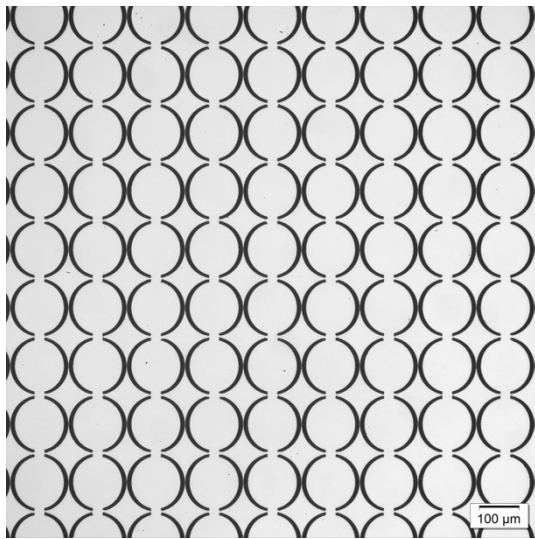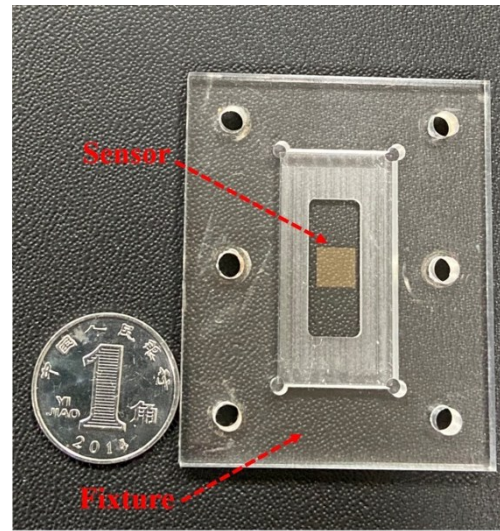
(a)
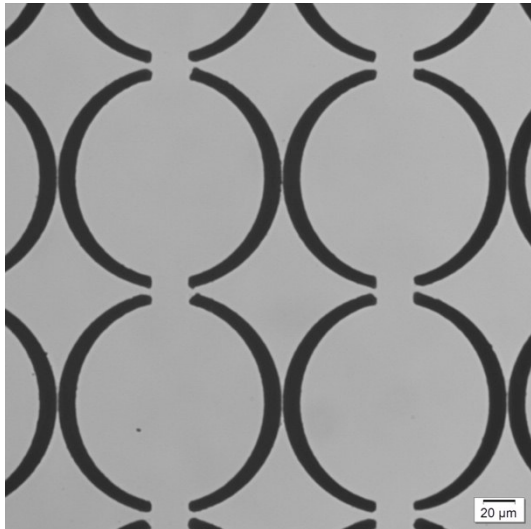
(b)

Fig. 3　The optical microscopy images of the fabricated metamaterial sensor (a) array structure of SRR, (b) single structure of SRR
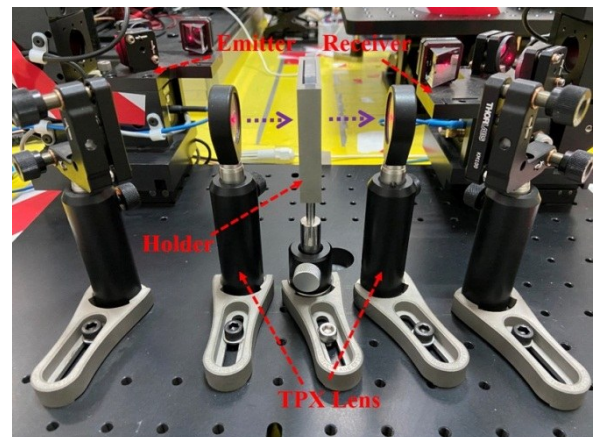图 3　加工的超材料传感器的光学显微图像(a)SRR 的阵列结构,(b)SRR 的单个结构

(a)

(b)

Fig. 4　(a) Sensor assembled with fixture, (b) measurement platform of the THz-TDS system
图 4　(a) 与夹具组装的传感器,(b) THz-TDS 系统测试平台

sorption by the water；finally，the sensor was mounted at normal incidence to the THz beam for spectrum collection. After the measurement，the metamaterial sensor coated with samples was rinsed thoroughly with deionized water and dried in drying oven again. The measurement for the clean and dry metamaterial sensor was taken before next deposition of the sample in order to ensure that the metamaterial was completely clean and there was no change in its optical properties. In addition，special attention was taken to ensure that each transmission spectrum was measured from the fixed location with the metamaterial sensor before and after depositing sample in order to avoid the measurement error. Three times of whole

measurement setups have been implemented for each sample to reduce the random error.

2　Results and discussions

2.1　Sensing characteristics of the metamaterial sensor

The whole SRR resonant unit can be regarded as an LC resonant circuit，the resonance frequency of which is defined as $f = 1/2\sqrt{LC}$ where C and L are the capacitance and inductance of the SRR metamaterial sensor，respectively. Our previous work[27] has shown that the resonance frequency of the LC circuit model is strongly dependent on the capacitance of the dielectric over-layer coated on the sensor surface. Therefore，the resonance frequency changes when the refractive index of the sample changes. The resonance frequency shifts induced by

the dielectric over-layer are primarily due to the changes in the SRR capacitance.

To further characterize the SRR resonators and evaluate the property of the metamaterial sensor，the frequency-dependent transmission of the sensor has been simulated by using the Computer Software Technology（CST） Microwave Studio. The results show that all transmittance spectra of the sensor coated with samples are shifted toward lower frequency regime with the increase of the refractive index of samples. The gaps in SRR structure behave like capacitors in the *LC* circuit which have resonant frequencies depending on the refractive index of surrounding materials. Thus，it can be possible to detect the refractive index of sample coated on the metamaterial sensor by monitoring the resonance frequency shifts. In the simulation，samples with the same refractive index and different thicknesses have been used to represent the samples with different concentrations. The transmission spectra of metamaterial for different refractive indexes with the sample thickness of 0. 4 μm are shown in Fig. 5 （a）. The relationship between frequency shift and refractive index is shown in Fig. 6（a），the results show that the frequency shift changes linearly with the refractive index value changing from 1. 0 to 2. 4 in an incremental step of 0. 2. The transmission spectra of SRR with the same refractive index of 1. 2 and different thicknesses are shown in Fig. 5（b）. The relationship between frequency shift and the thickness of sample film is shown in Fig. 6 （b），The results show that the frequency shift changes linearly with the thickness change from 0. 4 μm to 2. 4 μm in incremental steps of 0. 4 μm. The sensitivity of the SRR metamaterial sensor has been calculated，reaching 32. 0 GHz/RIU and 46. 0 GHz/RIU for the sample thickness of 0. 4 μm and 0. 8 μm，respectively. Hence， we realized qualitative and quantitative sensing of the sample concentration by using the proposed SRR metamaterial sensor.

2. 2　Performance analysis of the fabricated metamaterial sensor

The concentration dependent characteristics of the fabricated SRR metamaterial sensor have been investigated in this section. As mentioned above，the metamaterial sensor is sensitive to the relative index and the thickness of the sample solution coated on the surface. The resonant frequency will get red shift when the relative index and thickness of the solution sample increase，which means the sensor can be used for detecting solution sample with different relative indexes and different concentrations.

The positions of resonant peaks' shift as the concentrations of IS，LC，and TR solutions change，as shown in Fig. 7（a-c）. To observe more details，the region 0. 90- 1. 02 THz is magnified. As shown in Fig. 7，the position of the resonant peak shifts from 0. 980 THz to 0. 950 THz，0. 980 THz to 0. 958 THz and 0. 980 THz to 0. 961 THz as the concentration of IS，LC and TR changes from 0 to 4 mg/ml，respectively. The corresponding measurement sensitivity is 48. 6 GHz/RIU，47. 5 GHz/RIU and 37. 6 GHz/RIU，respectively. The positions of resonant
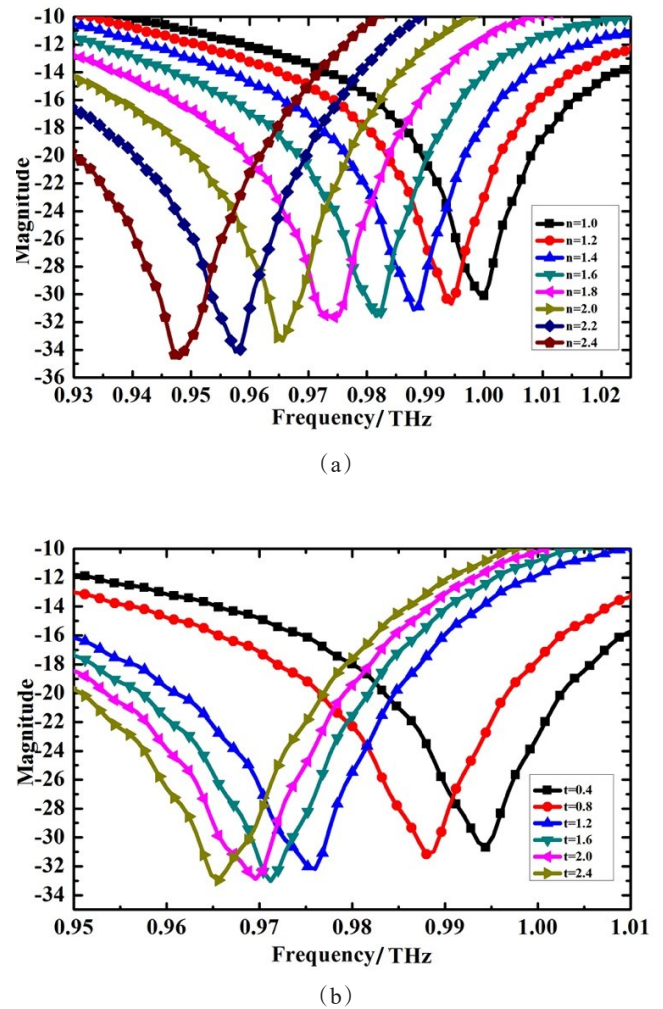

（a）

（b）

Fig. 5　（a）Simulated transmission spectra of metamaterial sensor for different refractive index analyte with the thickness of 0.4 μm， （b）simulated transmission spectra of metamaterial sensor for different thickness analyte with the refractive index of 1.2
图5　（a）具有不同折射率，厚度为0.4 μm的分析物透射光谱仿真结果图，（b）不同厚度，折射率为1.2的分析物透射光谱仿真结果图

peaks are all red shifted with the increase of the sample solution concentrations，which agrees very well with the simulations. Moreover，Fig. 7（a）shows that the resonant peaks of IS solutions to concentrations of 0. 2 mg/ml and 0. 4 mg/ml are almost the same，which means the minimum detectable IS concentration of our proposed metamaterial sensor is determined to be 0. 4 mg/ml due to the frequency resolution of the TDS system is 10 GHz. Similarly，Fig. 7（b）shows that the minimum detectable LC concentration of our proposed metamaterial sensor is determined to be 0. 2 mg/ml，as the resonant peaks of 0. 2 mg/ml and 0. 4 mg/ml are different. While Fig. 7 （c）shows that the minimum detectable TR concentration of our proposed metamaterial sensor is determined to be 2 mg/ml in our experiment，as the resonant peaks of 0. 4 mg/ml，0. 2 mg/ml and 0 mg/ml are the same. Fig. 7（a-c）experimentally show how the transmittance spectra of
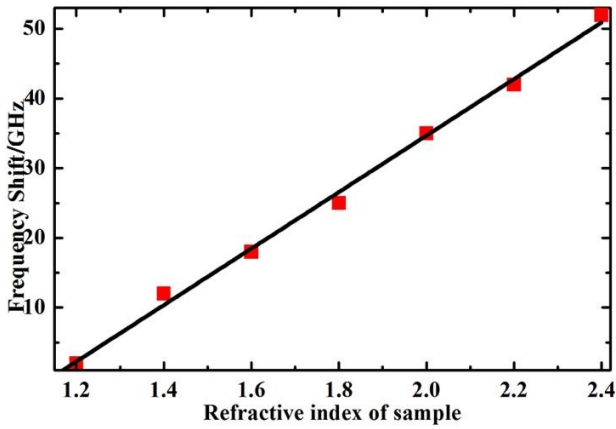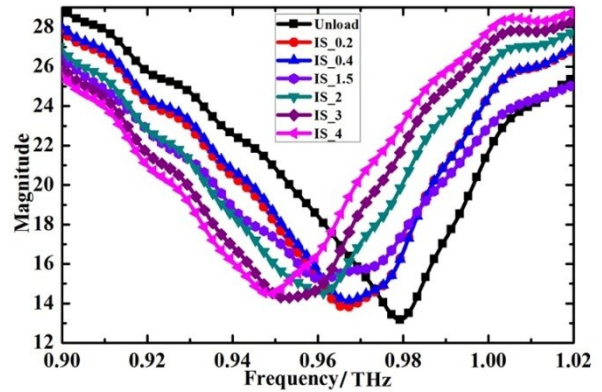
(a)
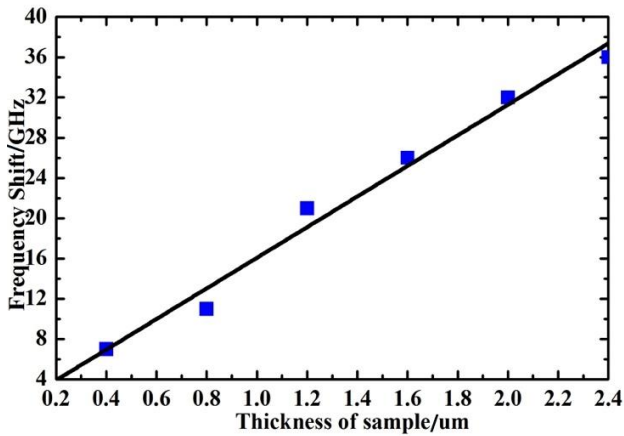
(b)

Fig. 6 (a) and (b) represent the relationship between frequency shift and refractive index and the relationship between frequency shift and the thickness of sample film, respectively
图6 （a）和（b）分别代表了频率偏移与折射率之间的关系和频率偏移与样品薄膜厚度之间的关系

the metamaterial sensor changed with the concentration of IS, LC and TR ranging from 0.2 mg/ml to 4 mg/ml. The transmittance spectra of each concentration could be well-distinguished from each other at the resonance frequency peaks when the IS and LC was under consideration. When the sensor was coated with TR solution samples, the transmittance spectra could not be distinguished clearly.

For further study, the frequency shift values of the resonant peaks versus solution concentrations were plotted in Fig. 8. The experimental results agreed to well with the simulation results. The clear linear relationships between the frequency shift values and the concentration of IS and LC were observed and a fitting model for them was built, as indicated by the line in Fig. 8. The frequency shift values increased as the concentration increased, and the fitting equation was estimated to be：
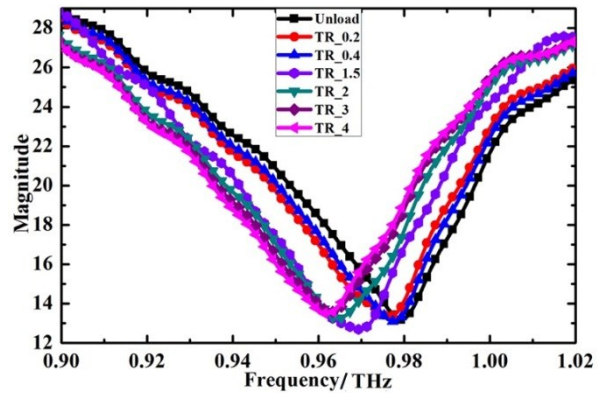
$$\Delta f = k*\rho + m \qquad , \quad (1)$$

(a)
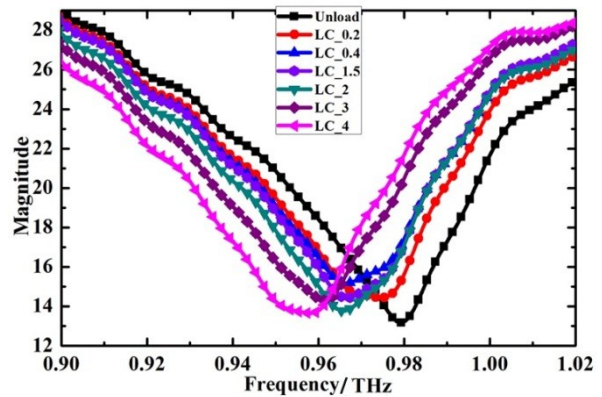
(b)

(c)

Fig. 7 (a), (b) and (c) represent the measured transmission spectra of inositol (IS), leucine (LC), and taurine (TR) with different concentrations, respectively
图7 （a）,（b）和（c）分别代表测量得到的不同浓度的肌醇（IS）、亮氨酸（LC）和牛磺酸（TR）透射光谱图

where ρ is the concentration of solution samples in mg/ml, k and m are the fitting coefficients. The fitting coefficients k and m for IS and LC solution sample are 4.71 and 10.98, 3.73 and 6.35, respectively. These results
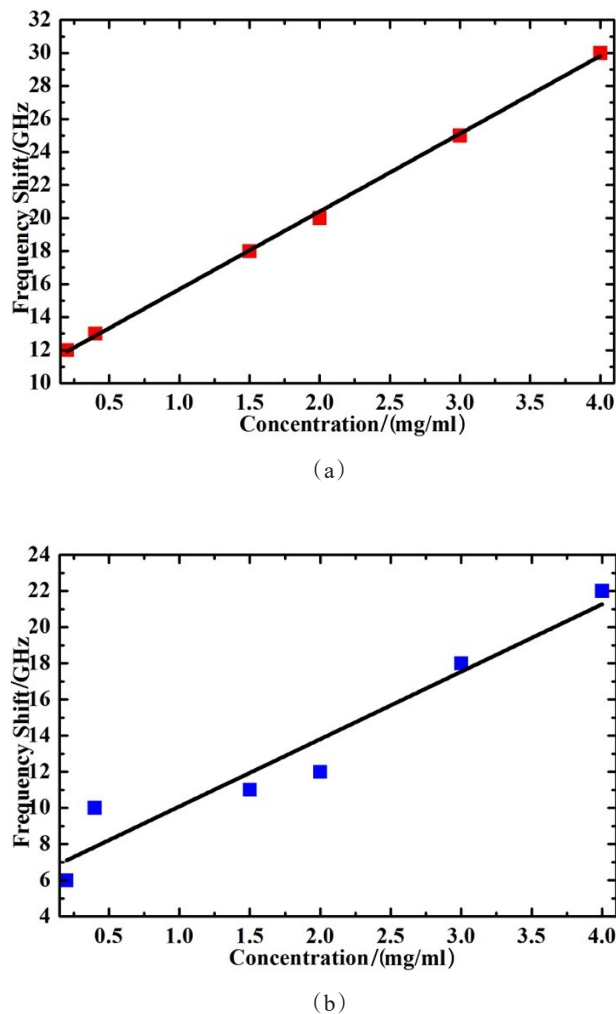
(a)

(b)

Fig. 8   (a) and (b) represent the relationship between frequency shift and concentration of inositol (IS) and leucine (LC) solution changing from 0.2 to 4 mg/ml, respectively

图 8 （a）和（b）分别表示肌醇（IS）和亮氨酸（LC）溶液浓度在 0.2~4 mg/ml 时对应的频率偏移关系图

indicate that the concentration of solution samples could be predicted based on the different frequency shift, which means the quantitative analysis of sample could be achieved.

In addition, selective detection of proposed metamaterial sensor for different samples with the same concentration has been studied, and the results were shown in Fig. 9. The black line represents a sensor without any samples. The samples with concentration of 4 mg/ml were successively coated on the sensor surface, and the transmittance spectra were obtained. The green, blue and red lines represent the transmission spectra of IS, LC and TR, respectively. There was a significant difference in the transmittance spectra, because the characteristic frequency of IS is closer to the resonant frequency of the SRR sensor than the characteristic frequency of LC and TR, which means higher resonant coupling strength. Furthermore, the SRR sensor can be specifically de-

signed for other target samples by simply changing its structural parameters to make the resonant frequency of the SRR overlap spectral with the characteristic frequency of the target samples. These features are attractive in the field of biological, chemical and food industry.
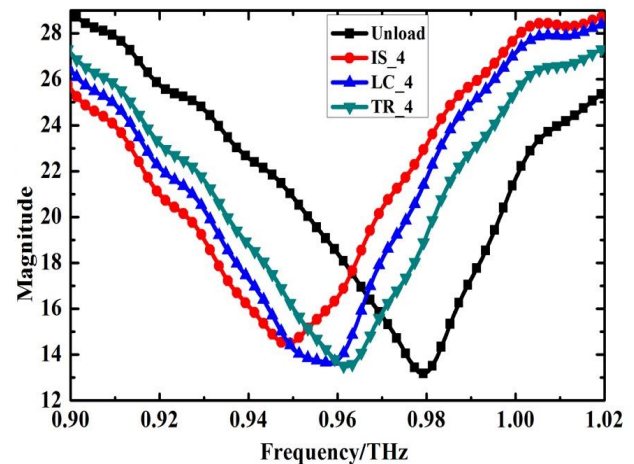

Fig. 9   The measured transmission spectra of inositol (IS), leucine (LC), and taurine (TR) with the solution concentration of 4 mg/ml

图 9   测量得到的浓度为 4 mg/ml 的肌醇（IS）亮氨酸（LC）和牛磺酸（TR）透射光谱图

3   Conclusion

In short, we have proved the feasibility of detecting food additives based on a metamaterial sensor in the terahertz range both theoretically and experimentally. The common additives such as inositol(IS), LC and TR have been sensed as examples. The results show that the proposed metamaterial sensor can effectively detect concentration of LC as low as 0. 2 mg/ml. The proposed detection method is based on the principle that samples of different thicknesses cause different frequency shifts, and it has its positive side and negative one. The positive side was that this approach could be universally applied to other food additives or even biological materials; while the negative one was that the precision and accuracy of the measured results were quite sensitive to the deposition of any non-target samples. Therefore, we must prevent the metamaterials from being contaminated by the non-target samples during the sample preparation and measurement. The detection method with the advantage of simple operation and low cost, which provides an effective reference for realizing the application of metamaterial in the field of food safety in the future.

References

［1］Tao H, Strikwerda A C, Liu M, *et al*. Performance enhancement of terahertz metamaterials on ultrathin substrates for sensing applications［J］. *Applied Physics Letters*, 2010, **97**(26): 261909.

［2］O'Hara J F, Singh R, Brener I, *et al*. Thin-film sensing with planar terahertz metamaterials: sensitivity and limitations［J］. *Optics Express*, 2008, **16**(3): 1786-1795.

［3］George P A, Hui W, Rana F, *et al*. Microfluidic devices for terahertz spectroscopy of biomolecules［J］. *Optics Express*, 2008, **16**

（3）：1577-1582.

［4］Qin J, Xie L, Ying Y. Determination of tetracycline hydrochloride by terahertz spectroscopy with PLSR model［J］. *Food chemistry*, 2015, **170**: 415-422.

［5］Gu H, Shi C, Wu X, *et al*. Molecular methylation detection based on terahertz metamaterial technology［J］. *Analyst*, 2020, **145**（20）: 6705-6712.

［6］Wang Y, Zhao Z, Qin J, *et al*. Rapid in situ analysis of l-histidine and α-lactose in dietary supplements by fingerprint peaks using terahertz frequency-domain spectroscopy［J］. *Talanta*, 2020, **208**: 120469.

［7］Withayachumnankul W, Jaruwongrungsee K, Tuantranont A, *et al*. Metamaterial-based microfluidic sensor for dielectric characterization［J］. *Sensors and Actuators A: Physical*, 2013, **189**: 233-237.

［8］Nazarov M M, Cherkasova O P, Shkurinov A P. A comprehensive study of albumin solutions in the extended terahertz frequency range［J］. *Journal of Infrared, Millimeter, and Terahertz Waves*, 2018, **39**（9）: 840-853.

［9］Shin H J, Jang H W, Ok G. Highly sensitive detection of 4-Methylimidazole using a terahertz Metamaterial［J］. *Sensors*, 2018, **18**（12）: 4304.

［10］Hafez H A, Chai X, Ibrahim A, *et al*. Intense terahertz radiation and their applications［J］. *Journal of Optics*, 2016, **18**（9）: 093004.

［11］Son J H. Terahertz electromagnetic interactions with biological matter and their applications［J］. *Journal of Applied Physics*, 2009, **105**（10）: 102033.

［12］Siegel P H. Terahertz technology in biology and medicine［J］. *IEEE transactions on microwave theory and techniques*, 2004, **52**（10）: 2438-2447.

［13］Castañeda-Ovando A, de Lourdes Pacheco-Hernández M, Páez-Hernández M E, *et al*. Chemical studies of anthocyanins: A review［J］. *Food chemistry*, 2009, **113**（4）: 859-871.

［14］Carocho M, Barreiro M F, Morales P, *et al*. Adding molecules to food, pros and cons: A review on synthetic and natural food additives［J］. *Comprehensive reviews in food science and food safety*, 2014, **13**（4）: 377-399.

［15］Bearth A, Cousin M E, Siegrist M. The consumer's perception of artificial food additives: Influences on acceptance, risk and benefit perceptions［J］. *Food quality and preference*, 2014, **38**: 14-23.

［16］Bennett M, Onnebo S M N, Azevedo C, *et al*. Inositol pyrophosphates: metabolism and signaling［J］. *Cellular and Molecular Life Sciences*, 2006, **63**（5）: 552-564.

［17］Wilson M S C, Livermore T M, Saiardi A. Inositol pyrophosphates: between signalling and metabolism［J］. *Biochemical Journal*, 2013, **452**（3）: 369-379.

［18］Gu C, Mao X, Chen D, *et al*. Isoleucine plays an important role for maintaining immune function［J］. *Current Protein and Peptide Science*, 2019, **20**（7）: 644-651.

［19］Ge Z D, Pravdic D, Bienengraeber M, *et al*. Isoflurane Postconditioning Protects against Reperfusion Injury by Preventing Mitochondrial Permeability Transition by an Endothelial Nitric Oxide Synthase – Dependent Mechanism［J］. *The Journal of the American Society of Anesthesiologists*, 2010, **112**（1）: 73-85.

［20］Imaki H, Jacobson S G, Kemp C M, *et al*. Retinal morphology and visual pigment levels in 6-and 12-month-old rhesus monkeys fed a taurine‐free human infant formula［J］. *Journal of neuroscience research*, 1993, **36**（3）: 290-304.

［21］Hernández-Benítez R, Vangipuram S D, Ramos-Mandujano G, *et al*. Taurine enhances the growth of neural precursors derived from fetal human brain and promotes neuronal specification［J］. *Developmental neuroscience*, 2013, **35**（1）: 40-49.

［22］Cataldi T R I, Telesca G, Bianco G, *et al*. Quantitative determination of taurine in real samples by high-performance anion-exchange chromatography with integrated pulsed amperometric detection［J］. *Talanta*, 2004, **64**（3）: 626-630.

［23］Baranda A B, Jiménez R M, Alonso R M. Simultaneous determination of five 1, 4-dihydropyridines in pharmaceutical formulations by high-performance liquid chromatography – amperometric detection［J］. *Journal of Chromatography A*, 2004, **1031**（1-2）: 275-280.

［24］Mohammadi A, Rezanour N, Dogaheh M A, *et al*. A stability-indicating high performance liquid chromatographic（HPLC）assay for the simultaneous determination of atorvastatin and amlodipine in commercial tablets［J］. *Journal of chromatography B*, 2007, **846**（1-2）: 215-221.

［25］Islam M A, Mahbub P, Nesterenko P N, *et al*. Prospects of pulsed amperometric detection in flow-based analytical systems-a review［J］. *Analytica chimica acta*, 2019, **1052**: 10-26.

［26］Guo J, Shi Y, Xu C, *et al*. Quantification of plasma myo-inositol using gas chromatography – mass spectrometry［J］. *Clinica Chimica Acta*, 2016, **460**: 88-92.

［27］Ma J, Wang S, Yang Y, *et al*. Simulation of terahertz-band metamaterial sensor for thin film analyte detection［J］. *AIP Advances*, 2020, **10**（8）: 085227.